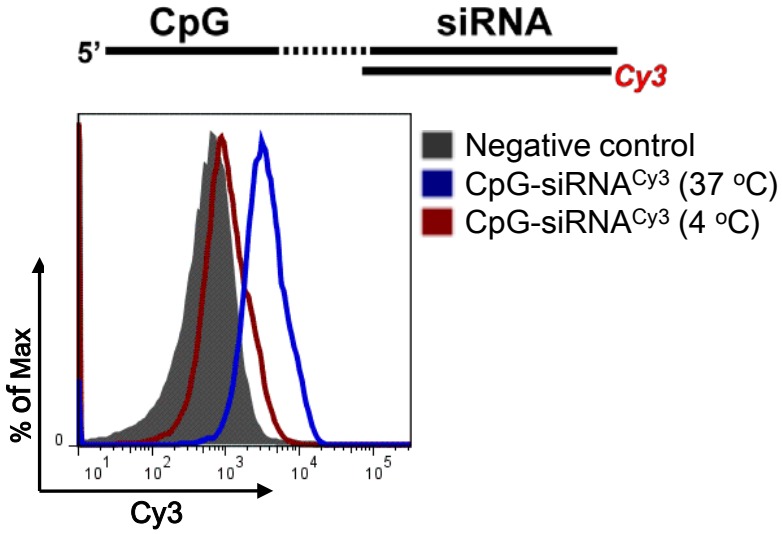

Supplementary Figure 1. CpG-siRNA is actively internalized by target immune cells under normal physiological conditions. Shown is the uptake of CpG-*Stat3* siRNA$^{5'SS\text{-}Cy3}$ by RAW 264.7 macrophages at 37 ^{o}C and 4 ^{o}C as measured by flow cytometry.

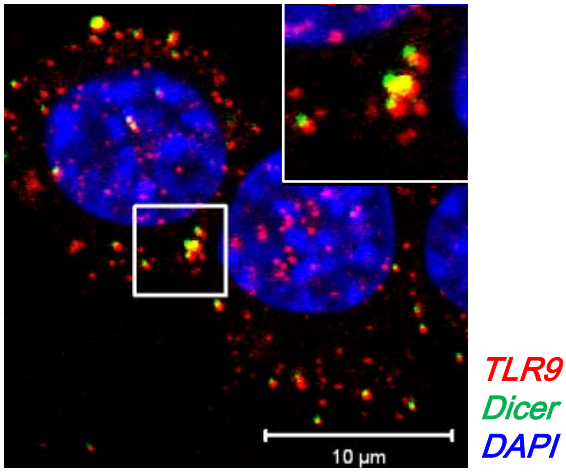

Supplementary Figure 2. TLR9 and Dicer are found in similar intracellular compartments in RAW 264.7 macrophages under basal conditions. Confocal microscopy; Scale bar: 10 µm.

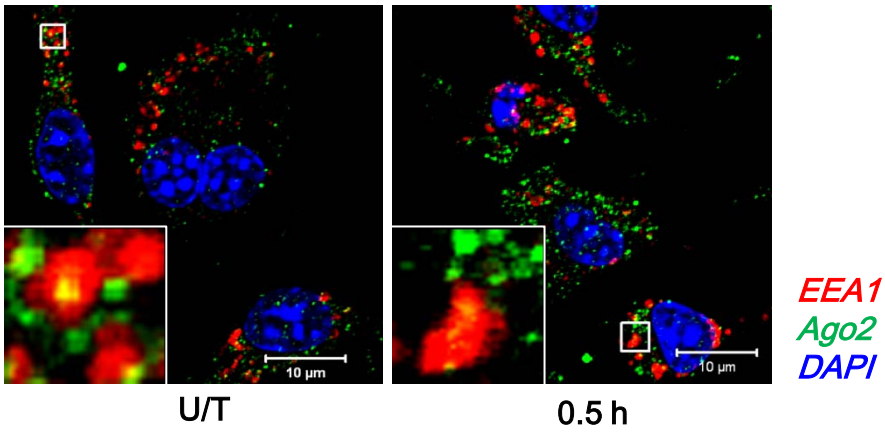

Supplementary Figure 3. Ago2 is detectable on a fraction of early endosomes regardless of cell treatment with CpG-siRNA. DAPI was used for nuclear staining. Shown are confocal microscopy images acquired from primary mouse bone marrow-derived macrophages. Scale bars: 10 µm.

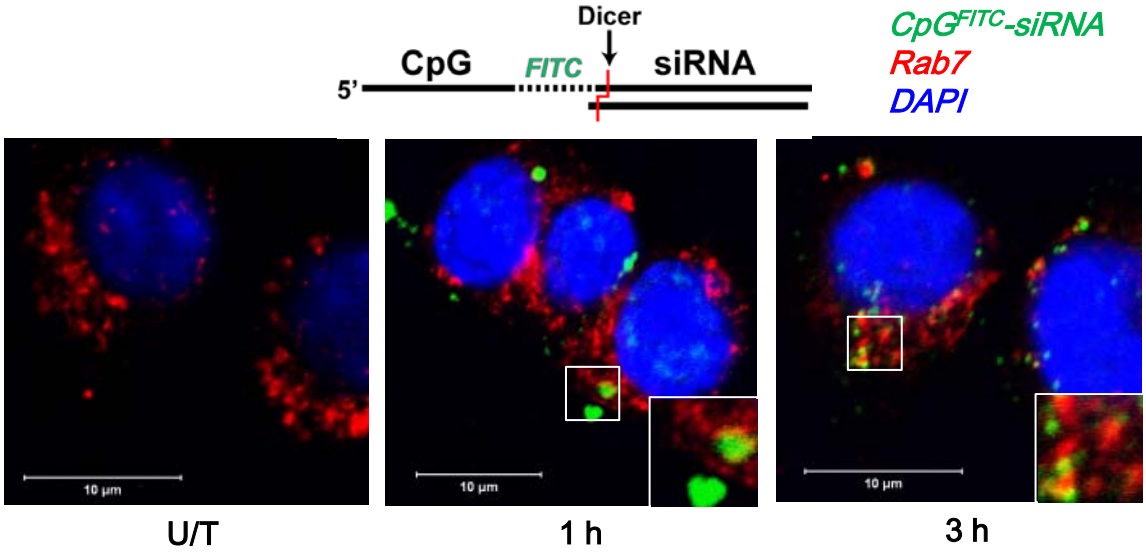

Supplementary Figure 4. The uncoupled CpG part of the conjugate remains in maturing endosomes. RAW 264.7 macrophages were treated with CpG^{FITC}–siRNA for indicated times. Cells were then fixed for the detection of late endosomes using Rab7-specific antibodies and analyzed by confocal microscopy. DAPI was used for nuclear staining. Scale bars: 10 µm.

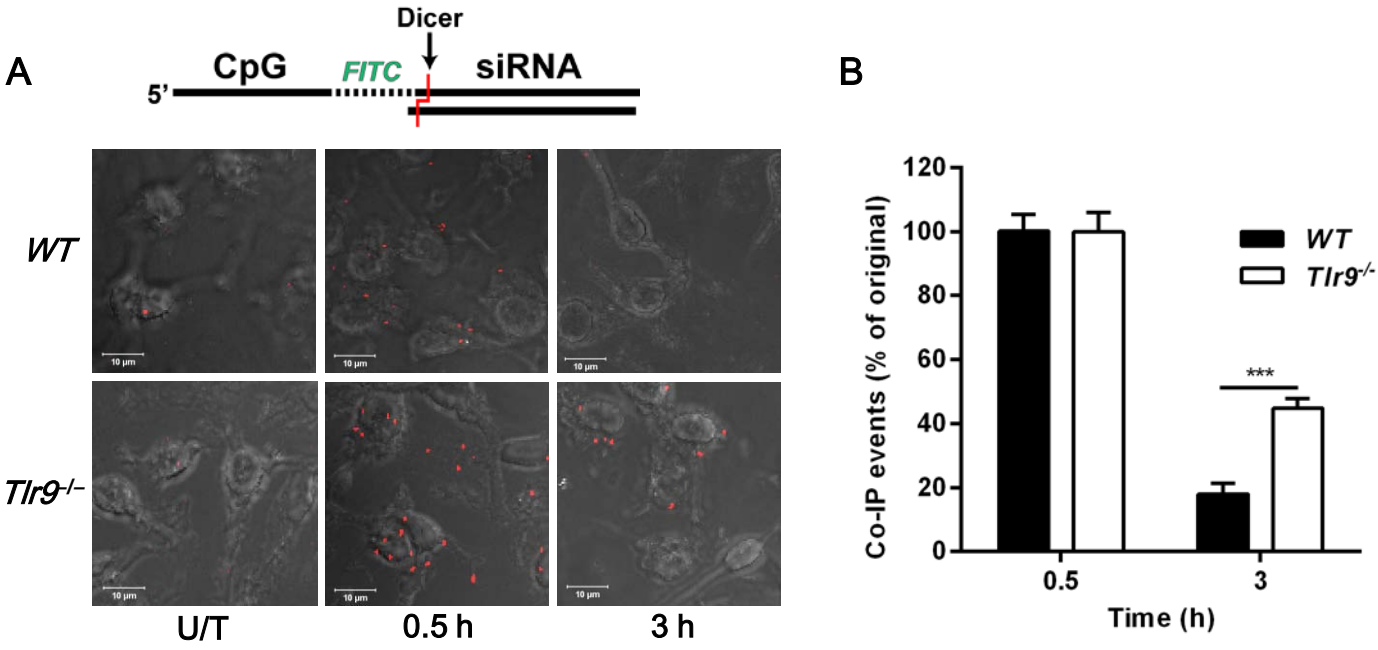

Supplementary Figure 5. Lack of TLR9 extends the interaction between CpG-siRNA and Dicer endonuclease. Bone-marrow derived macrophages from WT or *Tlr9*$^{-/-}$ mice were incubated with CpG^{FITC}–siRNA for indicated times. Cells were fixed, and the interaction between CpG^{FITC}-siRNA and Dicer was detected by *in situ* proximity ligation assay with FITC- and Dicer-specific antibodies. Shown are confocal microscopy images (Z stack projections; scale bars: 10 μm) (A), and the average counts of colocalization events per cell normalized to that at 0.5 h; mean ±SEM (B).

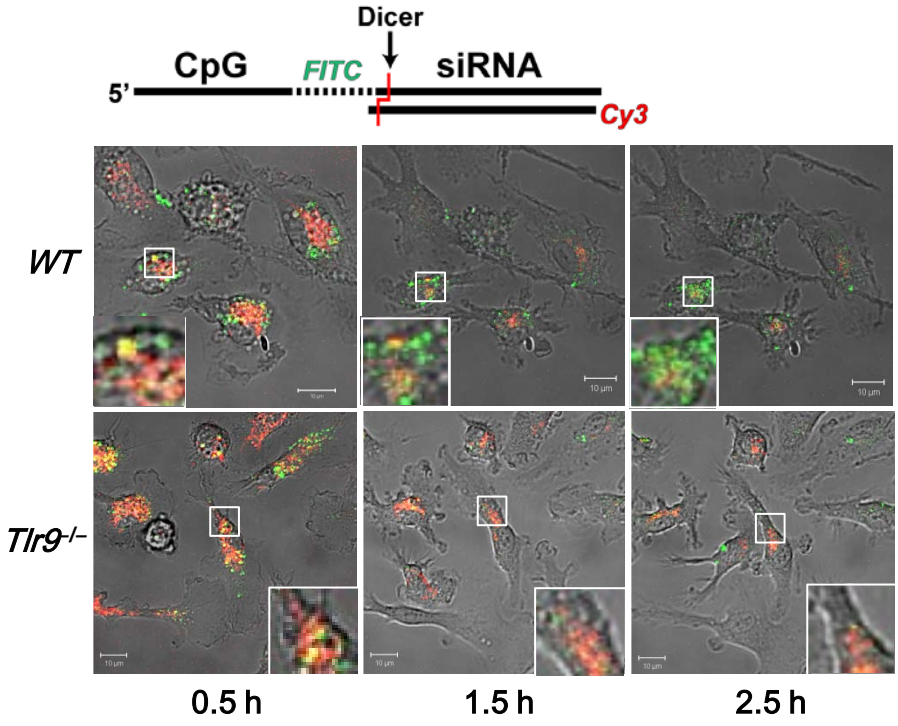

Supplementary Figure 6. The uncoupling of CpG-siRNA and endosomal release of the diced siRNA is delayed in *Tlr9*-deficient cells. Confocal microscopy in living WT (top row) and *Tlr9*$^{-/-}$ (bottom row) primary bone marrow-derived macrophages incubated with CpG^{FITC}-siRNA$^{5'SS\text{-}Cy3}$ for 20 min, washed and imaged for indicated times. Single Z layers, scale bars: 10 μm. Shown are the results from one of three independent experiments.

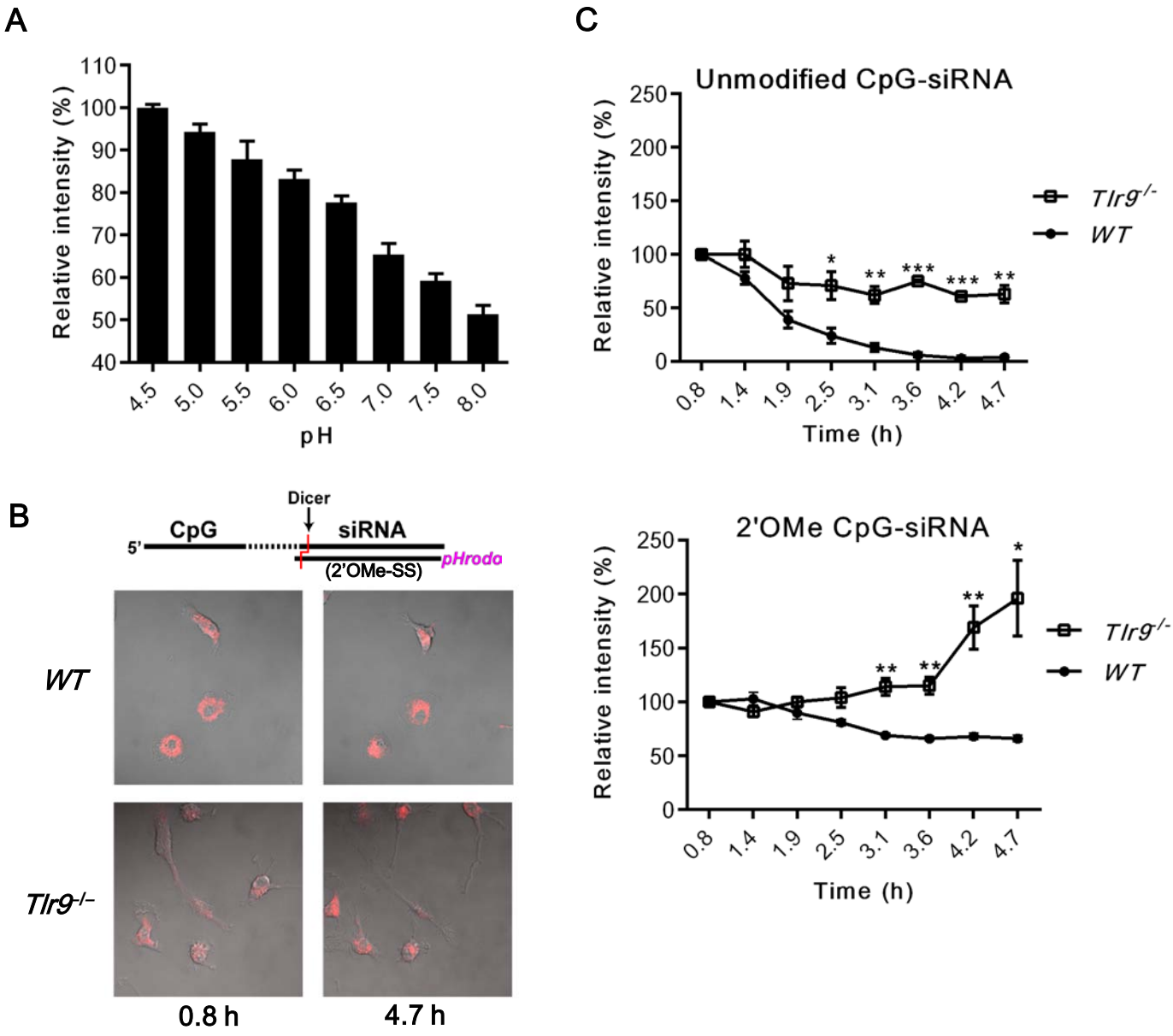

Supplementary Figure 7. TLR9 is required for siRNA release from early endosomes. (A) pH calibration curve for pHrodo succinimidyl ester in series of citric buffers with pH ranging from 4.5 to 8.0. Representative experiment, run in quadruplicates, mean ±SEM. (B) Representative images from time-lapse confocal microscopy in living WT and *Tlr9* $^{-/-}$ BMDM treated with CpG-*Stat3* siRNA$^{5'SS\text{-}pHrodo}$ fully modified with 2'OMe at siRNA SS. (C) Relative intensity of pHrodo emission as a function of time in WT and *Tlr9* $^{-/-}$ BMDM treated with unmodified and SS-2'OMe CpG-siRNA. Top panel is reproduced from Fig. 6B to allow for a comparative analysis of data obtained from cells treated with two types of CpG-siRNA constructs.

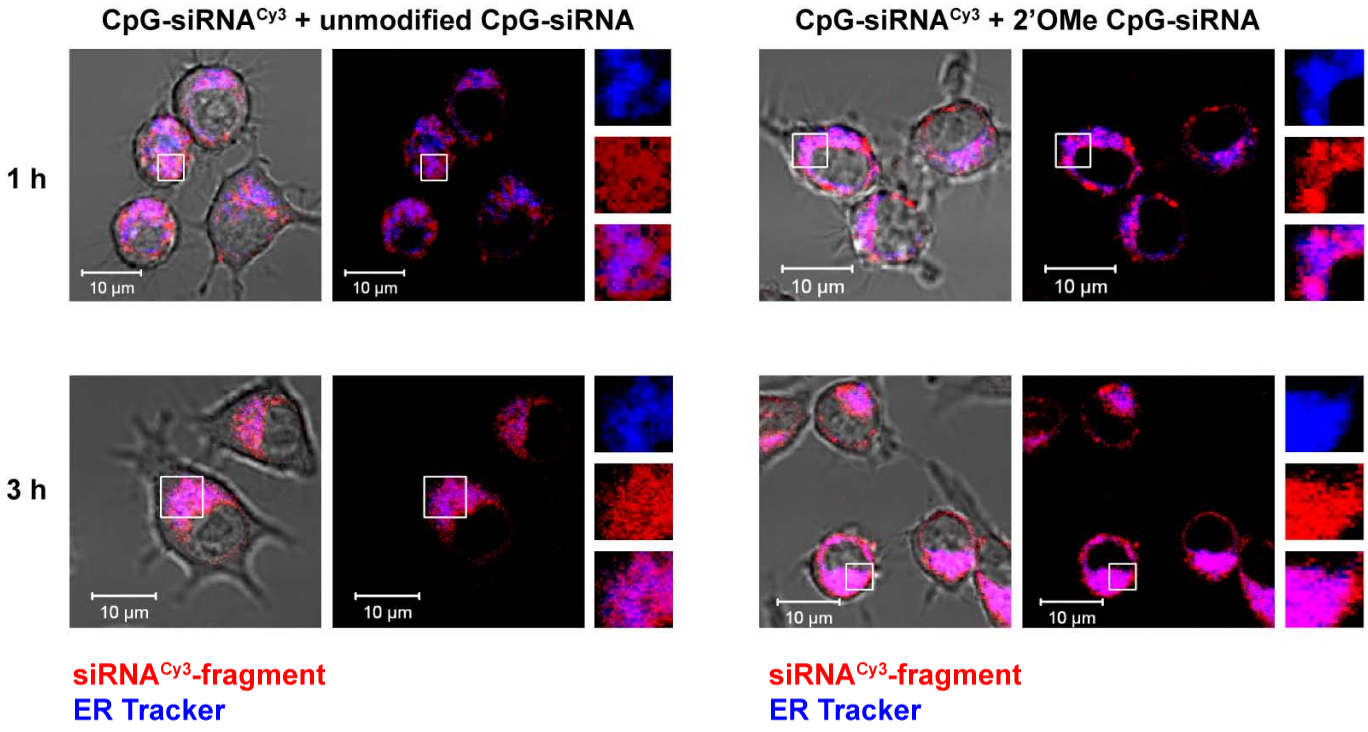

Supplementary Figure 8. Translocation of the diced siRNA from EE to ER is not affected by inhibiting TLR7 using 2'OMe-modified oligonucleotides. Confocal microscopy in live RAW 264.7 cells treated with equimolar mixture of CpG-Stat3 siRNA$^{5'SS\text{-}Cy3}$ with unmodified (left panels) and fully 2'OMe-modified antisense strand (right panels) for 3 h. After incubation, cells were stained using green ER Tracker (pseudocolored blue).

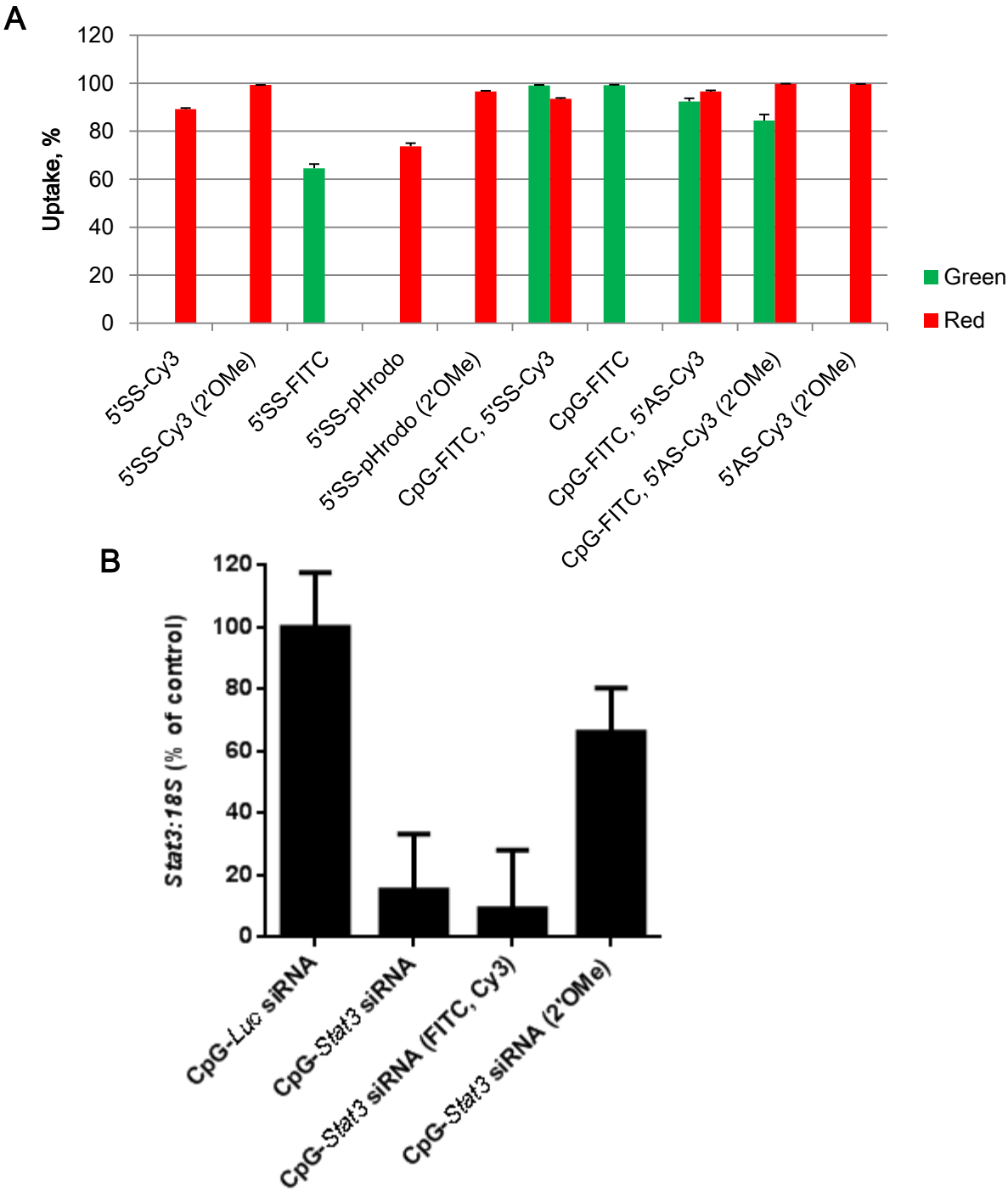

Supplementary Figure 9. Conjugation of various fluorochromes to CpG-siRNA does not influence conjugate uptake and target gene silencing. (A) RAW 264.7 macrophages were incubated for 3 h with various CpG-*Stat3* siRNA conjugates fluorescently labeled as indicated (FITC = green; Cy3, pHrodo = red). The percentage of cells that internalized conjugates were assessed using flow cytometry. Shown are means ±SEM (n = 3). (B) *Stat3* gene silencing in primary WT mouse macrophages is unaffected by conjugation of CpG-siRNA to FITC and Cy3 but it is impaired by 2'OMe-modification of both strands in the siRNA. Shown are real-time qPCR results with *Stat3* expression level in CpG-*Luc* siRNA-treated cells set as 100%. Shown are means ±SD (n = 3).

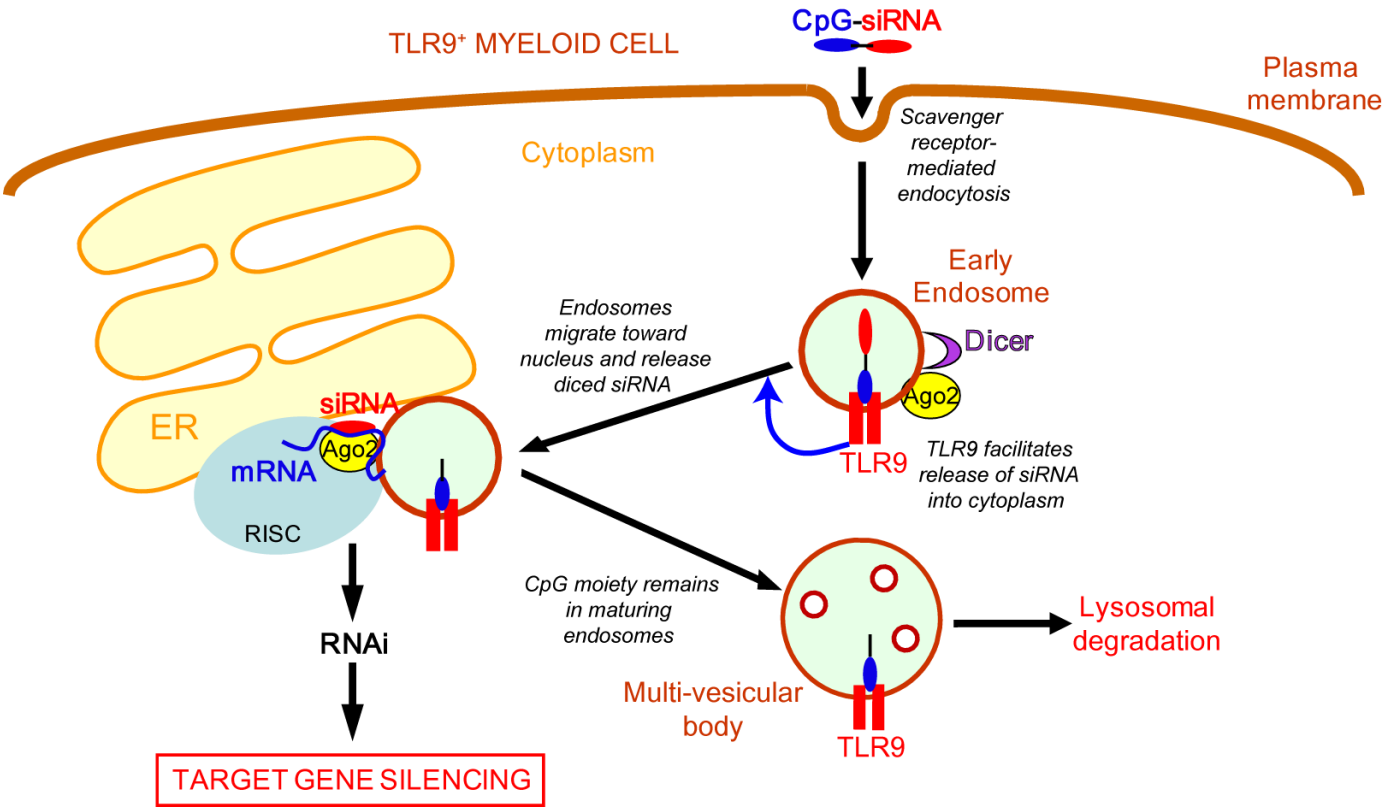

Supplementary Figure 10. The proposed mechanism of action of CpG-siRNA. The conjugate is taken up by scavenger receptor-mediated endocytosis into early endosomes, and binds to TLR9. Then 21-mer fragment of the siRNA is separated from the conjugate with involvement of Dicer residing within early endosomes. TLR9 facilitates siRNA release from early endosomes and its translocation into RISC complexes localized in cytoplasm or on the ER. Simultaneously with those processes, endosomes migrate toward the perinuclear ER, where the released siRNA can be incorporated into Ago2 to finalize the assembly of RISC complex and initiate RNA interference. After siRNA is released, the cleaved CpG moiety remains in maturating endosomes which move away from ER, fuse to lysosomes, and degrade their content.